

ARTICLE OPEN



cAMP-mediated upregulation of HCN channels in VTA dopamine neurons promotes cocaine reinforcement

Lianwei Mu^{1,4}, Xiaojie Liu^{1,4}, Hao Yu¹, Casey R. Vickstrom^{1,3}, Vladislav Friedman¹, Thomas J. Kelly¹, Ying Hu¹, Wantang Su^{1,2}, Shuai Liu¹, John R. Mantsch¹ and Qing-song Liu¹✉

© The Author(s) 2023

Chronic cocaine exposure induces enduring neuroadaptations that facilitate motivated drug taking. Hyperpolarization-activated cyclic nucleotide-gated (HCN) channels are known to modulate neuronal firing and pacemaker activity in ventral tegmental area (VTA) dopamine neurons. However, it remained unknown whether cocaine self-administration affects HCN channel function and whether HCN channel activity modulates motivated drug taking. We report that rat VTA dopamine neurons predominantly express *Hcn3-4* mRNA, while VTA GABA neurons express *Hcn1-4* mRNA. Both neuronal types display similar hyperpolarization-activated currents (I_h), which are facilitated by acute increases in cAMP. Acute cocaine application decreases voltage-dependent activation of I_h in VTA dopamine neurons, but not in GABA neurons. Unexpectedly, chronic cocaine self-administration results in enhanced I_h selectively in VTA dopamine neurons. This differential modulation of I_h currents is likely mediated by a D_2 autoreceptor-induced decrease in cAMP as D_2 (*Drd2*) mRNA is predominantly expressed in dopamine neurons, whereas D_1 (*Drd1*) mRNA is barely detectable in the VTA. Moreover, chronically decreased cAMP via Gi-DREADD stimulation leads to an increase in I_h in VTA dopamine neurons and enhanced binding of HCN3/HCN4 with tetratricopeptide repeat-containing Rab8b-interacting protein (TRIP8b), an auxiliary subunit that is known to facilitate HCN channel surface trafficking. Finally, we show that systemic injection and intra-VTA infusion of the HCN blocker ivabradine reduces cocaine self-administration under a progressive ratio schedule and produces a downward shift of the cocaine dose-response curve. Our results suggest that cocaine self-administration induces an upregulation of I_h in VTA dopamine neurons, while HCN inhibition reduces the motivation for cocaine intake.

Molecular Psychiatry (2023) 28:3930–3942; <https://doi.org/10.1038/s41380-023-02290-x>

INTRODUCTION

Hyperpolarization-activated cyclic nucleotide-gated (HCN) channels are activated by membrane hyperpolarization and gated by cAMP [1, 2]. cAMP binding to a cyclic nucleotide binding domain (CNBD) of the HCN channel facilitates channel opening by shifting the threshold for activation to more depolarized membrane potentials and accelerating the kinetics of channel activation [3, 4]. cAMP-mediated modulation of HCN gating regulates many important processes; for example, β -adrenergic agonists increase heart rate by facilitating HCN activation in sinoatrial node cells [5, 6]; α_2A -adrenergic tone in the prefrontal cortex strengthens working memory by decreasing cAMP gating of HCNs [7], and it reduces stress responses via the same mechanism in the bed nucleus of the stria terminalis [8]. cAMP modulation of HCN2 leads to neuronal hyperexcitability in nociceptors that transmit neuropathic pain [9]. These effects are mediated by acute neurotransmitter-mediated changes in cAMP and HCN gating. Much less is known about how chronic changes in cAMP affect HCN function. A recent study has shown that acute and chronic Gs-DREADD stimulation produced opposite modulation of HCN function in hippocampal CA1 pyramidal neurons via cAMP-dependent mechanisms [10]. Importantly, this mechanism may

explain the delayed therapeutic effects of monoaminergic antidepressants, which are known to chronically elevate cAMP [10]. In addition, chronic increase in intracellular cAMP drives diabetes-associated pain by facilitating HCN2 activation and action potential (AP) firing in nociceptors [11].

Dopamine neurons in the ventral tegmental area (VTA) regulate reward, decision making, stress resilience and drug addiction [12, 13]. AP firing in VTA dopamine neurons is governed by voltage-dependent conductances including HCN [13–15]. Dopamine neurons express $G\alpha_{i/o}$ -coupled D_2 dopamine autoreceptors that can be activated directly by dopamine or indirectly by cocaine [16–18]. Cocaine self-administration is expected to cause a chronic decrease in cAMP in dopamine neurons via D_2 autoreceptor activation, however, it remains unknown whether cocaine self-administration affects HCN function and whether HCN activity modulates motivated cocaine taking. In the present study, we first conducted RNAscope to determine the expression of all four HCN isoforms (*Hcn1-4* mRNA) in VTA dopamine and GABA neurons. Next, we investigated whether bidirectional changes in cAMP alter I_h in identified VTA dopamine and GABA neurons. Thirdly, we examined whether cocaine self-administration alters I_h in both neuronal types and whether

¹Department of Pharmacology and Toxicology, Medical College of Wisconsin, Milwaukee, WI 53226, USA. ²Department of Exercise Physiology, Beijing Sport University, Beijing 100084, China. ³Present address: Department of Neurology, Washington University School of Medicine, St. Louis, MO 63110, USA. ⁴These authors contributed equally: Lianwei Mu, Xiaojie Liu. ✉email: qslu@mcw.edu

Received: 12 February 2023 Revised: 25 September 2023 Accepted: 3 October 2023

Published online: 16 October 2023

chronic decreases in cAMP mediates I_h modulation. Finally, we studied whether VTA-specific and systemic administration of ivabradine affects cocaine self-administration. Here, we demonstrate that cocaine self-administration led to an upregulation of I_h in VTA dopamine neurons via cAMP-dependent mechanisms, and both intra-VTA and systemic injections of ivabradine reduced the motivation to self-administer cocaine. Thus, HCN blockers may offer a potential therapeutic approach for the treatment of cocaine use disorder. This is particularly relevant considering that the most common cause for mortality from long-term cocaine use is dilated cardiomyopathy-associated heart failure [19], and that ivabradine is a HCN blocker that is FDA-approved for the management of chronic heart failure [20, 21].

MATERIALS AND METHODS

Animals

Long-Evans rats were purchased from Envigo (Indianapolis, IN). Heterozygous TH-Cre [22] and homozygous tdTomato reporter rats were obtained from the Rat Resource & Research Center (RRRC, Columbia, MO) and were crossed to produce TH-tdTomato reporter rats. Roughly equal numbers of male and female rats (7–9-week-old at the beginning of experiments) were used. All protocols were approved by the Medical College of Wisconsin's Institutional Animal Care and Use Committee.

RNAscope in situ hybridization

Following transcardial perfusion with 4% paraformaldehyde, rat brains were extracted and rapidly frozen on dry ice. Coronal midbrain sections (15 μ m) were cut on a cryostat (Leica CM1860, Nussloch, Germany). Fluorescent probes targeting *Rattus norvegicus* mRNA (Advanced Cell Diagnostics Inc; Hayward, CA) were incubated with the sections per the manufacturer's directions and imaged using a Leica TCS SP8 confocal microscope. RNAscope was performed as described [23, 24]. The relative expression levels of mRNA that encode *Slc6a3*, *Gad1*, *Hcn1*, *Hcn2*, *Hcn3*, *Hcn4*, *Drd1* and *Drd2* in the VTA were quantified and compared using Imaris (Bitplane, Zürich, Switzerland).

Slice preparation and electrophysiology

Rats were anesthetized with isoflurane and transcardially perfused with NMDG-based solution [25, 26]. Brains were removed, trimmed, and embedded in low-gelling-point agarose. Horizontal VTA slices (200 μ m) were cut using a vibrating slicer (Leica VT1200s) in NMDG-based solution [25, 26]. Na^+ was gradually reintroduced [25, 26] and slices were allowed to rest in ACSF for at least an additional 30 min. Whole-cell recordings and protocols to measure I_h currents were conducted as described [27, 28].

Stereotaxic surgeries, AAV injections, and jugular catheterization

Prior to surgeries, rats were anesthetized with ketamine (90 mg/kg, i.p.) and xylazine (10 mg/kg, i.p.). For jugular catheterization, a round-tip polyurethane catheter (C30PU-RJV1611, Instech Laboratories, Inc, Plymouth Meeting, PA) was inserted into the right jugular vein. The catheter was connected to a vascular access button (22-gauge; VABR1B/22, Instech) and implanted subcutaneously on the back of the rats. Intravenous catheters were flushed with 0.2 ml of heparinized saline (30 units/ml) and cefazolin (100 mg/ml), and patency was tested by i.v. infusion of 0.05 ml xylazine (20 mg/ml) weekly or when a compromised catheter was suspected [29]. For stereotaxic surgery, rats were placed into Neurostar stereotaxic devices (Neurostar, Tübingen, Germany). For intra-VTA micro-injections, guide cannulae (26 gauge; P1 Technologies, Roanoke, VA) were implanted 2.8 mm above the VTA at stereotaxic coordinates: AP, -5.3 mm; ML ± 2.4 mm; DV, -7.8 mm; 10° angle [30, 31]. For DREADD experiments, a glass capillary Nanoinjector (Neurostar) and a Nanoject III Programmable Nano-liter Injector (Drummond Scientific Company, Broomall, PA) were used to inject AAV8-hSyn-DIO-hM4D(Gi)-mCherry or AAV8-hSyn-DIO-mCherry (250 nl each; Addgene, Watertown, MA) into the VTA of TH-Cre rats at the same coordinates. Rats received an analgesic injection (buprenorphine-SR, 1 mg/kg, s.c.) immediately following surgery. Rats were allowed for recovery of 1–2 weeks prior to the start of self-administration experiments.

Cocaine self-administration and yoked administration

Cocaine self-administration was conducted similarly to our previously published studies [25, 32]. Rats with no prior lever press training were placed into operant conditioning chambers (Med Associates Inc., Fairfax, VT) and allowed to self-administer cocaine for 10 days in 3 h sessions. Active responses resulted in a cocaine infusion and illumination of a cue light above the active lever for 5 s, followed by a 10 s timeout during which active responses were recorded but did not result in further infusions. Responding was maintained at fixed ratio 1 (FR1, 1 mg/kg/infusion) on days 1–5 and fixed ratio 2 (FR2, 0.5 mg/kg/infusion) on days 6–10. Rats that did not acquire stable self-administration after 10 days were excluded. Timepoints of cocaine infusions from rats that successfully acquired stable self-administration were used to yoke the delivery of i.v. saline, cocaine, or deschloroclozapine (DCZ) in additional cohorts of rats. One day following self-administration or yoked administration, slices were prepared for patch-clamp electrophysiology, as described above.

Additional cohorts of rats were used for testing the effects of intra-VTA infusion or systemic injection of ivabradine on FR2, FR2 multiple-dose and progressive ratio (PR) schedules. For intra-VTA infusion of ivabradine, the day following completion of self-administration training, vehicle (0.5 μ l/side) or ivabradine (25 or 50 ng/0.5 μ l/side) were bilaterally microinjected into the VTA via injector cannulae (33-gauge; P1 Technologies, Roanoke, VA). Cocaine self-administration was tested 10 min later. For i.p. ivabradine, rats first received i.v. injection of elacridar (5 mg/kg) followed by i.p. injection of ivabradine (3 or 10 mg/kg) or vehicle (0 mg/kg). Cocaine self-administration was tested 10 min later.

Co-Immunoprecipitation (Co-IP) reactions

Rats were deeply anesthetized with isoflurane, decapitated, and the coronal midbrain was cut using a rat brain matrix. Bilateral VTA was punched out and flash frozen. Co-IP reactions were performed with a commercial kit (26149, ThermoFisher, Rockford, IL) using anti-HCN3 (APC-057) or anti-HCN4 antibodies (APC-052, both from Alomone labs, Jerusalem, Israel).

Chemical reagents

ZD7288, (RS)-(\pm)-sulpiride, rolipram, forskolin and ivabradine hydrochloride were purchased from Tocris Bioscience (Ellisville, MO). DCZ dihydrochloride (water soluble) was purchased from Hello Bio Inc. (Princeton, NJ). Elacridar hydrochloride was purchased from Medchemexpress LLC (Monmouth Junction, NJ). Cocaine HCl was provided by the NIDA Drug Supply Program. All other common chemicals were obtained from Sigma-Aldrich (St. Louis, MO).

Statistics

Data are presented as the mean \pm SEM. Animal numbers and sample sizes are calculated based on statistical power analysis ($\alpha = 5\%$, Power = 0.8). For behavioral tests, prior to statistical testing equal variance was determined with Levene's test, normality was assessed with the Shapiro-Wilk test using OriginPro. Data sets were compared with either Student's *t*-test, Paired *t*-test, one-way ANOVA followed by Tukey's *post hoc* analysis, two-way repeated measures (RM) ANOVA, Kruskal-Wallis one-way ANOVA on ranks followed by Dunn's *post hoc* analysis for pair-wise comparisons, or the Kolmogorov-Smirnov test (*K-S* test). *Post hoc* analyses were performed only when ANOVA yielded a significant main effect or a significant interaction between the two factors. Results were significant at $p < 0.05$.

RESULTS

Differential expression of *Hcn1–4* mRNA in VTA dopamine and GABA neurons

HCN channels are assembled predominantly as heterotetramers from four subunits encoded by *Hcn1–4* [1, 33, 34]. Brain-wide in situ hybridization has shown that *Hcn1–4* mRNA is expressed in the VTA in adult rat brain [35]. Immunohistochemistry has shown that HCN2 is expressed in the rat VTA [36], and HCN4 is expressed in VTA dopamine and GABA neurons [37]. However, previous studies have not directly compared the expression of HCN channel isoforms in specific VTA cell types systematically. We conducted RNAscope in situ hybridization to assess the cell-type distribution of all four *Hcn* isoforms in the VTA. *Hcn1* and *Hcn2* mRNA were

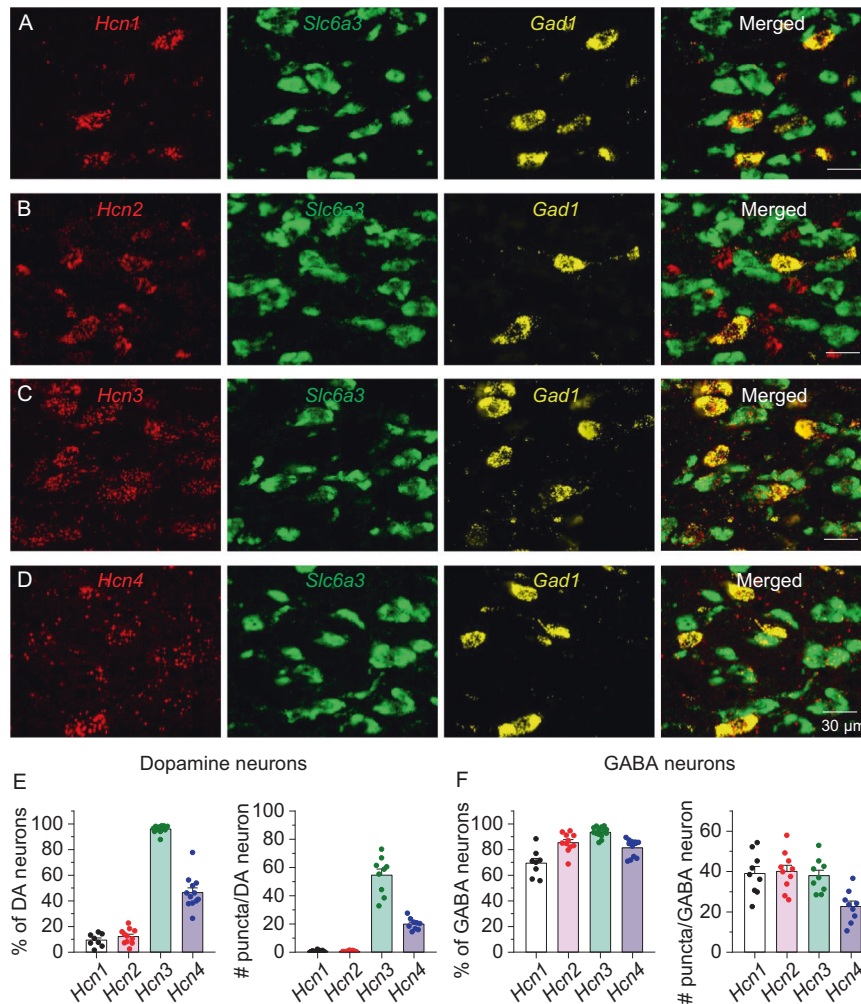


Fig. 1 Expression of *Hcn1–4* mRNA in rat VTA dopamine and GABA neurons. Representative 63x images of VTA sections labeled with RNAscope in situ hybridization for *Hcn1–4* (red), *Gad1* (GABA neuron, yellow) and *Slc6a3* (dopamine neuron, green) mRNA. **A, B** *Hcn1* and *Hcn2* mRNA were highly expressed in *Gad1* neurons, but barely detectable in *Slc6a3* neurons. *Hcn2* mRNA was also expressed on a cell type that remains to be detected. **C, D** *Hcn3* and *Hcn4* mRNA were expressed in both *Gad1* neurons and *Slc6a3* neurons. **E** Left, percentage of VTA dopamine neurons co-expressing *Hcn1–4* (*Hcn1*: 208 of 2245 neurons; *Hcn2*: 286 of 2350 neurons; *Hcn3*: 1591 of 1661 neurons; *Hcn4*: 1109 of 2392 neurons). Right, the number of *Hcn1–4* mRNA puncta expressed in VTA dopamine neurons. **F** Left, percentage of VTA GABA neurons co-expressing *Hcn1–4* (*Hcn1*: 428 of 619 neurons; *Hcn2*: 628 of 736 neurons; *Hcn3*: 509 of 545 neurons; *Hcn4*: 514 of 634 neurons). Right, the number of *Hcn1–4* mRNA puncta expressed in VTA GABA neurons. ($n = 8$ to 14 imaged sections from 4 rats).

expressed in $69.3 \pm 3.7\%$ and $85.3 \pm 2.2\%$ GABA neurons, respectively, as shown by colocalization with glutamic acid decarboxylase 1 (*Gad1*) mRNA, but these were rarely expressed in dopamine neurons (*Hcn1*, $9.3 \pm 1.7\%$; *Hcn2*, $12.2 \pm 1.8\%$) as defined by colocalization with solute carrier family 6 member 3 (*Slc6a3*, dopamine transporter, DAT) mRNA (Fig. 1A, B, E, F, Figs. S1, S2). *Hcn3* mRNA was expressed in $93.4 \pm 1.1\%$ GABA and $95.8 \pm 0.7\%$ dopamine neurons, *Hcn4* mRNA was expressed in $81.2 \pm 1.9\%$ GABA and $46.4 \pm 3.7\%$ dopamine neurons (Fig. 1C–F, Figs. S3, S4). Thus, VTA dopamine neurons express mainly *Hcn3–4* mRNA, while VTA GABA neurons express all four *Hcn* isoforms. Detailed statistics for this and subsequent results are described in figure legends.

***I_h* currents in VTA dopamine and GABA neurons are sensitive to cAMP**

Among HCN1–4, HCN2 and HCN4 are most sensitive to cAMP, while HCN1 and HCN3 show less cAMP sensitivity [3, 38, 39]. We recorded HCN currents (I_h) in identified dopamine and GABA neurons in the VTA. We labeled midbrain dopamine neurons with fluorescent reporter tdTomato by breeding tyrosine hydroxylase (TH)-Cre rats [22] with tdTomato reporter rats. Consistent with the

previous study [22], all tdTomato⁺ neurons colocalized with TH, but only $64.7 \pm 1.8\%$ TH⁺ neurons expressed tdTomato (Fig. S5). Thus, TH-tdTomato labeling of dopamine neurons is specific but incomplete. As tdTomato-negative neurons consisted of both GABA and dopamine neurons, we identified these neurons by collecting cytoplasmic mRNA for single-cell RT-PCR upon the completion of whole-cell recordings (Fig. S6). I_h currents were recorded as described [27]. Consistent with previous studies [37, 40], there were no significant differences of the I_h amplitude, membrane capacitance (C_m), and I_h current density and midpoint activation voltage ($V_{1/2}$) between VTA dopamine and GABA neurons (Fig. 2A–G). I_h currents in both dopamine neurons and GABA neurons were abolished by HCN blockers ZD7288 ($20 \mu\text{M}$) and ivabradine ($50 \mu\text{M}$) (data not shown). Bath application of the adenylyl cyclase activator forskolin ($20 \mu\text{M}$) and the phosphodiesterase-4 (PDE4) inhibitor rolipram ($1 \mu\text{M}$), which increased intracellular cAMP in the VTA [30, 41], induced similar depolarizing shifts of $V_{1/2}$ of I_h in VTA dopamine (Fig. 2H, I) and GABA neurons (Fig. 2J, K). These results are consistent with the expression of cAMP-sensitive HCN isoforms in both VTA dopamine (*Hcn4*) and GABA neurons (*Hcn2/Hcn4*) as revealed by RNAscope.

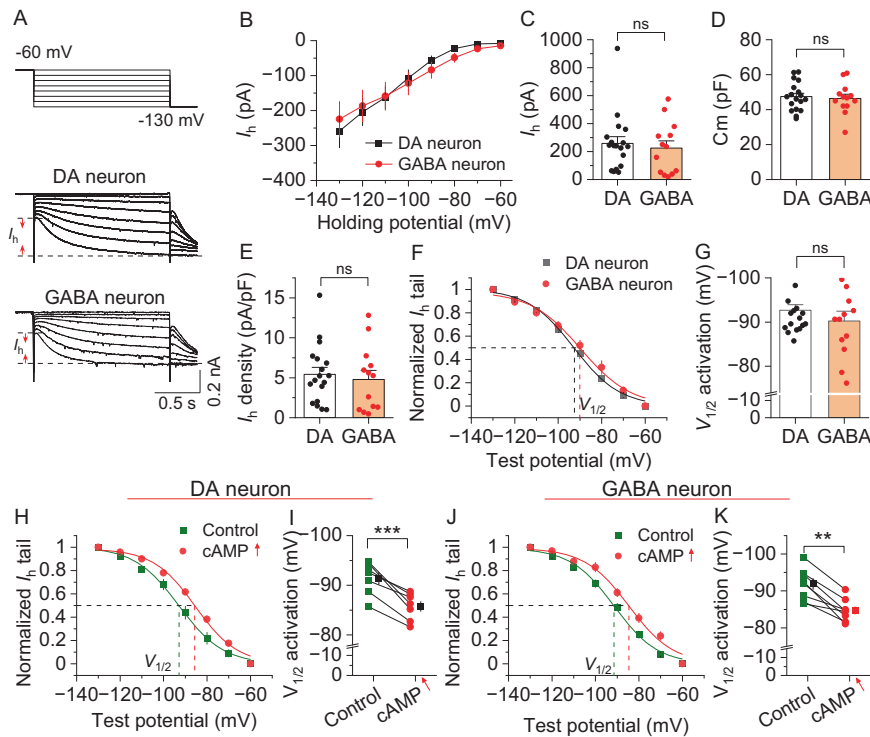


Fig. 2 I_h currents were not significantly different between VTA dopamine and GABA neurons and were sensitive to cAMP stimulation.

A Left: Voltage protocol for recording I_h current. Right: Representative I_h traces recorded from dopamine (DA) neurons and GABA neurons in the VTA. **B** There was no significant difference in I_h between dopamine and GABA neurons at all corresponding hyperpolarization potentials (two-way RM ANOVA, cell-type, $F_{1,29} = 0.02$, $p = 0.894$; holding potential, $F_{7,203} = 37.7$, $p < 0.001$; cell-type \times holding potential interaction, $F_{7,203} = 0.6$, $p = 0.770$; DA neuron, $n = 18$ cells; GABA neuron, 13 cells; $n = 4$ rats). **C** I_h amplitude was calculated by subtracting the instantaneous current from the steady-state current achieved during the voltage step at -130 mV, and no significant difference was detected (t -test, $t_{29} = 0.5$, $p = 0.640$, $n = 13$ –18 cells). **D** There was no significant difference in membrane capacitance (C_m) between dopamine and GABA neurons (t -test, $t_{29} = 0.4$, $p = 0.728$, $n = 13$ –18). **E** I_h current density ($=I_h$ amplitude at -130 mV/ C_m) was not significantly different between dopamine neurons and GABA neurons (t -test, $t_{29} = 0.5$, $p = 0.655$, $n = 13$ –18). **F** I_h activation curves in dopamine neurons and GABA neurons were generated by the tail current protocol. Tail current amplitudes were fitted with a Boltzmann function. **G** There was no significant difference in the midpoint activation voltage ($V_{1/2}$) between dopamine and GABA neurons (t -test, $t_{29} = 1.0$, $p = 0.322$). **H, I** Increasing cAMP (cAMP \uparrow) via bath perfusion of forskolin ($20 \mu\text{M}$) and rolipram ($1 \mu\text{M}$) led to a significant rightward shift in the I_h activation curve of a significant depolarizing shift in the $V_{1/2}$ of VTA dopamine neurons (paired t -test $t_6 = 6.4$, $p < 0.001$, $n = 7$ from 3 rats). **J, K** Increasing cAMP led to a significant depolarizing shift in the I_h activation curve and a depolarizing shift in the $V_{1/2}$ of VTA GABA neurons (paired t -test, $t_7 = 3.9$, $p = 0.006$, $n = 8$ from 3 rats). ns, not significant, $p > 0.05$, ** $p < 0.01$, *** $p < 0.001$.

Acute cocaine application modulated I_h in VTA dopamine neurons via D_2 autoreceptors

We next determined whether decreasing cAMP via $G_{\alpha i/o}$ -coupled dopamine D_2 receptors alters I_h currents in VTA dopamine neurons and GABA neurons. D_2 receptors are coupled to G protein-coupled inwardly rectifying potassium channels (GIRK) in midbrain dopamine neurons [42]. In the presence of the GIRK channel blocker BaCl_2 ($300 \mu\text{M}$), bath application of cocaine ($10 \mu\text{M}$) produced a hyperpolarizing shift of $V_{1/2}$ in VTA dopamine neurons (Fig. 3A, B), which was blocked by the D_2 receptor antagonist sulpiride ($1 \mu\text{M}$) (Fig. 3C, D). Cocaine did not significantly alter I_h in VTA GABA neurons (Fig. S7). RNAscope showed that dopamine receptor D_2 (*Drd2*) mRNA was expressed in virtually all dopamine neurons but only in $10.7 \pm 1.7\%$ GABA neurons (Fig. 3E, F, Fig. S8), which may explain why cocaine produced differential modulation of I_h in dopamine and GABA neurons. In contrast, D_1 (*Drd1*) mRNA was barely detectable in the VTA (Fig. 3G, Fig. S9) but *Drd1* mRNA clusters were detected in regions neighboring to the VTA (Fig. S9); In addition, *Drd1* and *Drd2* mRNA were abundantly expressed in the striatum with minimal overlap ($3.5 \pm 0.7\%$) (Fig. S10).

Chronic intravenous cocaine administration altered I_h currents and temporal summation of EPSPs in VTA dopamine neurons

We next investigated whether cocaine self-administration altered I_h currents in VTA dopamine and GABA neurons, which enabled us

to study how chronic changes in cAMP alter HCN function. Rats were trained to self-administer cocaine for 10 days, and separate groups of rats received saline or cocaine infusions yoked to the infusion schedule of previously self-administering rats. To determine whether cocaine self-administration decreases cAMP levels in the VTA, we used ELISA to measure cAMP levels from VTA tissue punches immediately after the last saline or cocaine administration. We found that cAMP levels in the VTA were decreased in rats that received yoked cocaine administration or cocaine self-administration compared to those in saline-administered rats (Fig. S11). Next, TH-tdTomato rats were trained for cocaine self-administration, yoked cocaine or saline administration for 10 days. Midbrain slices were prepared 1 day after the last cocaine or saline infusion (Fig. 4A). Compared with those of the yoked saline group, cocaine self-administration and cocaine yoked infusions led to significant increases in the amplitude and current density of I_h in VTA dopamine neurons (Fig. 4B–D, F). The changes in I_h in dopamine neurons cannot be attributed to a decrease in cell size, as membrane capacitance (C_m , Fig. 4E) and surface area of dopamine neurons (as determined by TH immunohistochemistry, Fig. S12) were not significantly different between the cocaine group and the yoked saline group. Cocaine self-administration and yoked cocaine infusions also produced a depolarizing shift of $V_{1/2}$ in VTA dopamine neurons (Fig. 4G, H). In contrast, cocaine self-administration did not change I_h amplitude,

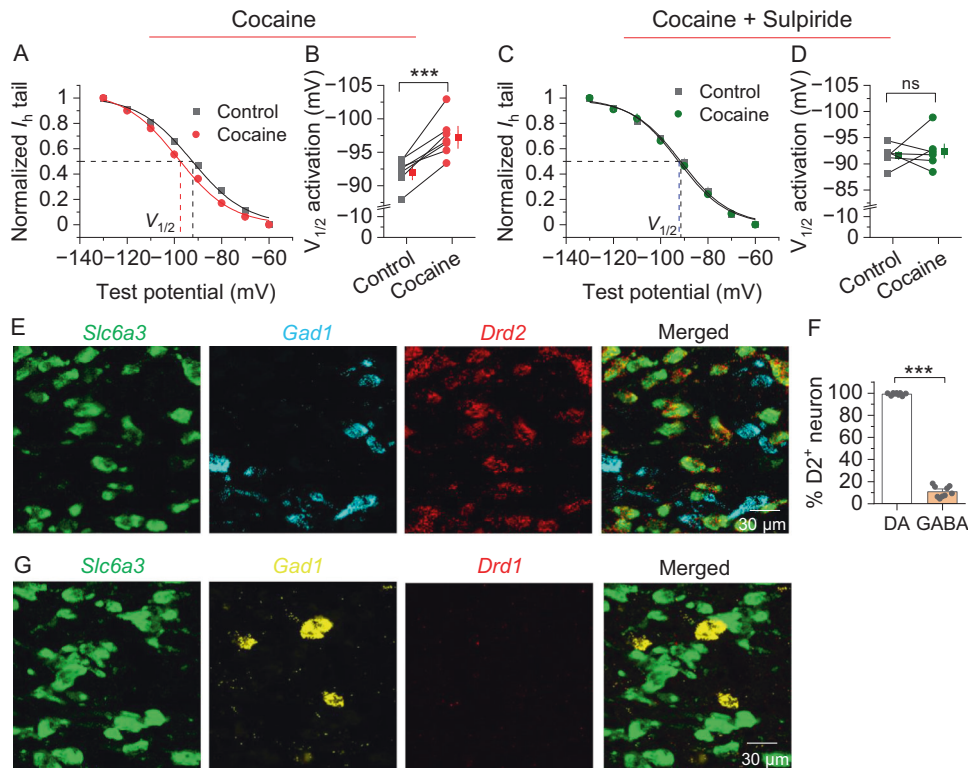


Fig. 3 Bath application of cocaine induced a hyperpolarizing shift of the $V_{1/2}$ of I_h currents in VTA dopamine neurons through activation of the D_2 -autoreceptor. **A, B** Bath perfusion of cocaine (10 μ M) induced a significant leftward shift in the I_h activation curve and a hyperpolarizing shift of the $V_{1/2}$ of VTA dopamine neurons (paired t -test, $t_6 = 6.3$, $p < 0.001$, $n = 7$ from 3 rats). **C, D** The shifts of cocaine on the I_h activation curve and the $V_{1/2}$ were blocked by D_2 receptor antagonist sulpiride (1 μ M) (paired t -test, $t_5 = 0.5$, $p = 0.641$, $n = 6$ from 3 rats). **E, F** $Drd2$ mRNA was abundantly expressed and completely colocalized with $Slc6a3$ mRNA but was expressed only in $\sim 10\%$ of GABA neurons (ns, not significant, $p > 0.05$, $***p < 0.001$; $n = 2$ rats). **G** $Drd1$ mRNA was barely detected in both dopamine and GABA neurons in the VTA ($n = 2$ rats).

I_h density and $V_{1/2}$ in VTA GABA neurons compared with the yoked saline group (Fig. 4J–M).

HCN activation at dendrites limits temporal summation of excitatory postsynaptic potentials (EPSPs) [10, 43, 44]. We next determined whether the cocaine-induced increase in I_h currents were associated with changes in temporal summation of EPSPs. EPSPs were evoked by a train of electrical stimulation (50 Hz \times 5) of excitatory synaptic inputs in the presence of a cocktail of GABA_A, GABA_B, D_2 and NMDA receptor antagonists. It is worth noting that VTA dopamine neurons typically exhibit tonic and bursting activity, with the latter characterized by phasic firing at a frequency range of 15–30 Hz [45]. This phasic firing can reach up to 60 Hz in stressed animals [46]. However, the choice of the 50 Hz stimulation frequency was not intended to mimic the in vivo firing patterns; rather, this high frequency stimulation has been commonly utilized in the assessment of the temporal summation of EPSPs, which indirectly reflects the strength of dendritic I_h [10, 43, 44]. Consistent with increased I_h , we found that VTA dopamine neurons in the cocaine self-administration and yoked cocaine groups exhibited significantly less temporal summation of evoked EPSPs compared with the yoked saline control, and ZD7288 induced a greater increase in temporal summation of EPSPs in the cocaine-exposed groups than that in the yoked saline group (Fig. 4).

HCN channels are important in governing pacemaker activity in midbrain dopamine neurons [13–15]. We examined whether cocaine self-administration was associated with changes in spontaneous AP firing in VTA dopamine neurons and whether ZD7288 affected AP firing. We found that cocaine self-administration led to a significant increase in spontaneous AP firing in VTA dopamine neurons compared to yoked saline

administration, and ZD7288 produced a greater suppression of spontaneous AP firing in cocaine group than that in saline group (Fig. S13). Thus, cocaine self-administration is accompanied by an increase in the activity of VTA dopamine neurons, ZD7288 reduces AP firing and abrogates the difference in AP firing between cocaine and saline groups.

Chronically decreased cAMP induced an up-regulation of I_h in VTA dopamine neurons

What might be the mechanism for the cocaine self-administration-induced differential modulation of I_h in dopamine and GABA neurons? D_2 ($Drd2$) mRNA was predominantly expressed in dopamine neurons, raising the possibility that a chronic decrease in cAMP via cocaine-induced D_2 receptor activation may underlie the I_h upregulation. Tetratricopeptide repeat-containing Rab8b-interacting protein (TRIP8b) is an auxiliary HCN channel subunit [47] responsible for HCN trafficking to the plasma membrane and enrichment at dendrites [44, 48]. TRIP8b competes with cAMP for binding of the CNBD of HCN channels, and chronic increased cAMP via Gs-DREADD stimulation was shown to disrupt TRIP8b binding and HCN surface trafficking in hippocampal CA1 pyramidal neurons [10]. Immunohistochemistry showed that TRIP8b was expressed in the VTA and colocalized with TH⁺ dopamine neurons (Fig. S14A). In the Allen Brain Atlas mouse in situ hybridization (ISH) database (<https://mouse.brain-map.org>), TRIP8b (also called Pex5l) is abundantly expressed in the VTA (Fig. S14B). One possibility is that the chronic decrease in cAMP during the 10-day cocaine self-administration or yoked cocaine infusions induced an enhanced TRIP8b binding with HCN channels and enhanced their surface trafficking, which provides a potential mechanism for the augmented I_h and dampened

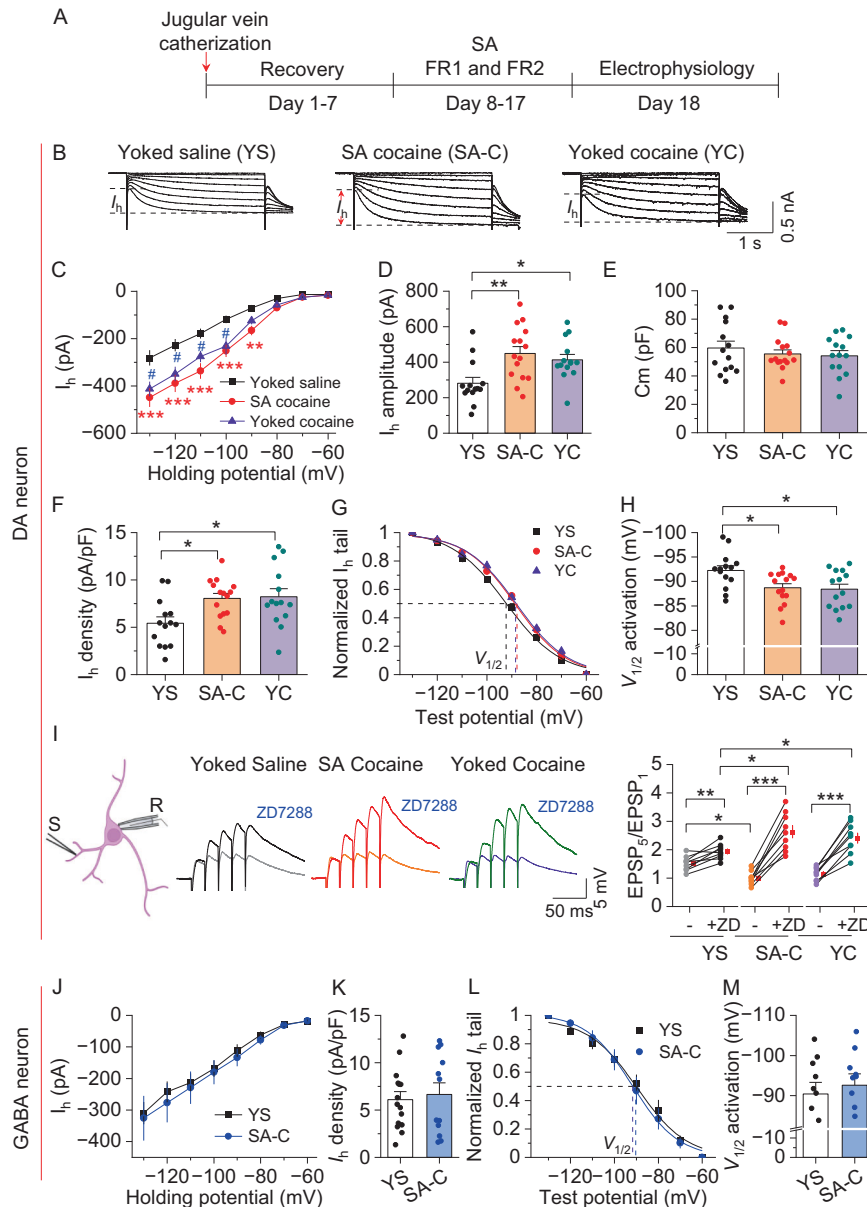


Fig. 4 Cocaine self-administration led to upregulation of I_h in VTA dopamine neurons. **A** Timeline of jugular vein catheterization, cocaine self-administration and electrophysiology. **B** Representative I_h currents recorded from VTA dopamine neurons after 10 days of yoked saline (YS), cocaine self-administration (SA) and yoked cocaine infusions (YC). **C** Compared with yoked saline infusions, cocaine self-administration and yoked cocaine infusions led to significant increases in I_h currents at corresponding hyperpolarization potentials (two-way RM ANOVA, Cocaine, $F_{2,40} = 8.6$, $p < 0.001$; holding potential, $F_{7,280} = 248.9$, $p < 0.001$; Cocaine \times holding potential interaction, $F_{14,280} = 5.5$, $p < 0.001$; $n = 14$ –15 from 5 rats; yoked saline vs cocaine SA, blue * and #, yoked saline vs yoked cocaine, red * and #; * $p < 0.01$, # $p < 0.001$). **D–F** Cocaine self-administration and yoked cocaine infusions led to significant increases in I_h amplitude (**D**; one-way ANOVA, $F_{2,42} = 6.5$, $p = 0.004$, $n = 14$ –15) and I_h density (**F**; one-way ANOVA, $F_{2,42} = 5.1$, $p = 0.010$, $n = 14$ –15 cells from 5 rats), but did not significantly change the membrane capacitance (C_m) of VTA dopamine neurons (**E**; one-way ANOVA, $F_{2,42} = 0.5$, $p = 0.587$, $n = 14$ –15 cells). **G, H** Cocaine self-administration and yoked cocaine infusions led to depolarizing shifts in the I_h activation curve the $V_{1/2}$ of VTA dopamine neurons (one-way ANOVA, $F_{2,42} = 4.9$, $p = 0.012$, $n = 14$ –15 cells). **I** Left: A schematic diagram shows the location of the stimulating electrode (S) and recording electrode (R). Representative EPSPs (50 Hz \times 5) showing temporal summation before and after application of ZD7288. Right: Comparison of changes in temporal summation of EPSPs (EPSP₅/EPSP₁ ratio) in cocaine self-administration, yoked cocaine and yoked saline groups in the absence and presence of ZD7288 (two-way RM ANOVA, Cocaine, $F_{2,24} = 0.2$, $p = 0.856$; ZD7288, $F_{1,24} = 172.0$, $p < 0.001$; Cocaine \times ZD7288 interaction, $F_{1,24} = 18.1$, $p < 0.001$; $n = 9$ cells from 4 rats). **J–M** Cocaine self-administration did not alter the I_h density (**J, K**; t -test, $t_{25} = 0.4$, $p = 0.716$) and $V_{1/2}$ (**L, M**; t -test, $t_{18} = 0.5$, $p = 0.597$) of GABA neurons in the VTA. For (**D–I**), * $p < 0.05$, ** $p < 0.01$, *** $p < 0.001$.

summation of EPSPs. To test the hypothesis, we investigated whether chronic Gi-DREADD stimulation via yoked delivery of deschloroclozapine dihydrochloride (DCZ) mimicked the effect of cocaine on I_h upregulation. DCZ is a highly brain-penetrant DREADD actuator that shows greater affinity and potency for DREADDs [49]. AAV8-hSyn-DIO-hM4D(Gi)-mCherry or the control

vector (AAV8-hSyn-DIO-mCherry) was injected into the VTA of TH-Cre rats (Fig. 5B, left). Two weeks after AAV expression, we examined the expression the AAVs in midbrain sections (Fig. 5A). The AAVs, as indicated by mCherry, were expressed in $79.9 \pm 4.2\%$ of TH⁺ dopamine neurons (green) but were not expressed in TH⁻ neurons in the VTA (Fig. 5B, right). Pressure ejection of DCZ (1 μ M)

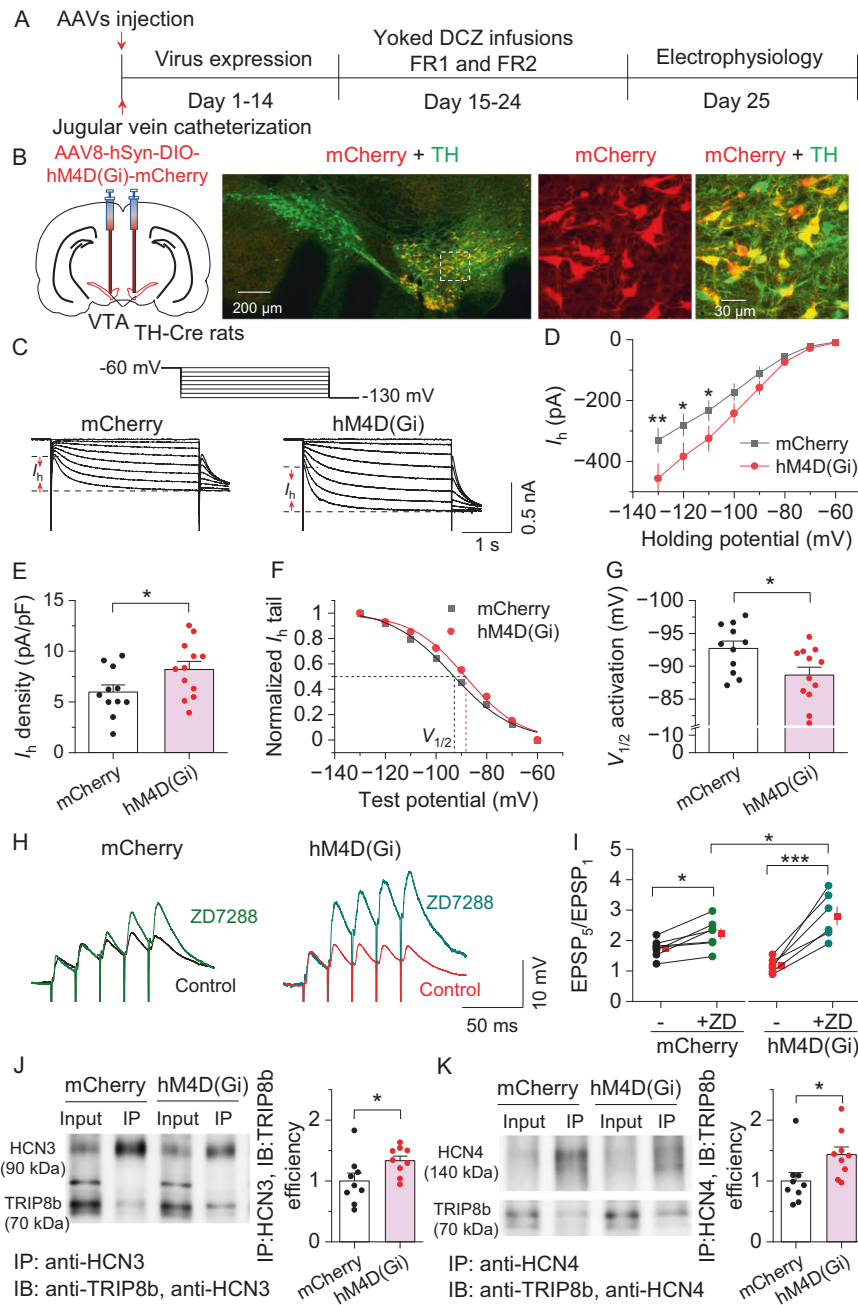


Fig. 5 Chronically decreasing cAMP with hM4D(Gi) induced an up-regulation of I_h in VTA dopamine neurons. **A** Timeline of viral injection, yoked DCZ infusions and electrophysiology. **B** AAV8-hSyn-DIO-hM4D(Gi)-mCherry [hM4D(Gi)] or AAV8-hSyn-DIO-mCherry (mCherry) was bilaterally microinjected into the VTA of TH-Cre rats. Immunohistochemistry showed that hM4D(Gi) was expressed in the majority of TH⁺ dopamine neurons (green) but was not expressed in TH⁻ neurons in the VTA of TH-Cre rats ($n = 5$ rats). **C** Representative I_h currents recorded from rats that received yoked DCZ infusions expressing mCherry or hM4D(Gi) in VTA dopamine neurons. **D** I_h amplitude was significantly increased in rats with expressing hM4D(Gi) compared to mCherry at the corresponding hyperpolarization potentials (two-way RM ANOVA, hM4D(Gi), $F_{1,21} = 2.7$, $p = 0.117$; holding potential, $F_{7,147} = 118.2$, $p < 0.001$; hM4D(Gi) \times holding potential interaction, $F_{7,147} = 3.1$, $p = 0.005$; $n = 11-12$ cells from 4 rats). **E** I_h current density was significantly increased in hM4D(Gi)-expressing rats compared with mCherry-expressing rats (t -test, $t_{21} = 2.1$, $p = 0.049$, $n = 11-12$ cells). **F, G** Yoked DCZ infusions led to a significant depolarizing shift of the $V_{1/2}$ in hM4D(Gi)-expressing rats compared to mCherry-expressing rats (t -test, $t_{21} = 2.4$, $p = 0.023$, $n = 11-12$ cells). **H** Representative temporal summation of evoked EPSPs (50 Hz \times 5) recorded from mCherry and hM4D(Gi)-expressing VTA dopamine neurons in TH-Cre rats that received yoked DCZ infusions. **I** Compared with mCherry-expressing VTA dopamine neurons, hM4D(Gi)-expressing dopamine neurons exhibited a smaller increase in temporal summation of EPSPs. ZD7288 induced greater increase in temporal summation of EPSPs in hM4D(Gi)-expressing rats (two-way RM ANOVA, hM4D(Gi), $F_{1,11} = 0.004$, $p = 0.856$; ZD7288, $F_{1,11} = 56.1$, $p < 0.001$; hM4D(Gi) \times ZD7288 interaction, $F_{1,11} = 16.4$, $p = 0.002$; $n = 6-7$ cells from 3 rats). **J, K** Representative Co-IP reaction was performed using anti-HCN3 (**J**) or HCN4 (**K**) antibodies in VTA lysate from rats that expressed mCherry and hM4D(Gi) in VTA dopamine neurons and received yoked DCZ administration. IP, immunoprecipitation; IB, immunoblotting. (HCN3: t -test, $t_{18} = 2.2$, $p = 0.044$, $n = 9$ and 9. HCN4: t -test, $t_{18} = 2.3$, $p = 0.034$, $n = 9$ and 9). For the entire figure, * $p < 0.05$, ** $p < 0.01$, *** $p < 0.001$.

via a patch pipette resulted in hyperpolarization and a pause of AP firing in hM4D(Gi)-expressing VTA dopamine neurons but did not affect AP firing in mCherry-expressing neurons (Fig. S15).

Next, hM4D(Gi)- or mCherry-expressing rats received 10 days of i.v. DCZ administration yoked to the infusion schedule of rats that self-administered cocaine. VTA slices or tissue punches were obtained one day after the last DCZ administration for electrophysiology and coimmunoprecipitation, respectively. Compared with those which received the mCherry control, I_h amplitude and I_h density were significantly increased in hM4D(Gi)-expressing VTA dopamine neurons (Fig. 5C–E), and there was a depolarizing shift of $V_{1/2}$ (Fig. 5F, G). hM4D(Gi)-expressing neurons exhibited dampened temporal summation of EPSPs (Fig. 5H, I), and the HCN blocker ZD7288 induced a greater increase in temporal summation of EPSPs in these neurons (Fig. 5H, I). Together, these results suggest chronic Gi-DREADD activation induces an upregulation of HCN function at somata and dendrites of VTA dopamine neurons. Finally, we investigated the mechanism that may underlie the upregulation of I_h induced by chronic hM4D(Gi) stimulation. We performed Co-IP using anti-HCN3 and -HCN4 antibodies as these HCNs are the main isoforms expressed in VTA dopamine neurons. We found that more TRIP8b bound to HCN3 or HCN4 in VTA tissue punches from rats that expressed hM4D(Gi) compared with rats that expressed the control vector mCherry following chronic yoked DCZ administration (Fig. 5J, K, Fig. S16). These results suggest that chronically decreased cAMP leads to increases in the TRIP8b-HCN interaction and surface trafficking of HCN channels.

Effects of intra-VTA infusions of ivabradine on cocaine self-administration

Does the upregulation of HCN function in VTA dopamine neurons contribute to motivated drug taking? To determine this, we examined whether intra-VTA infusion of ivabradine, a clinically approved HCN blocker [21], affected cocaine self-administration in rats. Rats were trained to self-administer cocaine under a fixed ratio-1 schedule (FR1, 1 mg/kg/infusion) for 5 days, followed by a FR2 schedule (0.5 mg/kg/infusion) for another 5 days (Fig. 6A). We found that bilateral intra-VTA infusions of ivabradine (25 and 50 ng/0.5 μ l/side) did not significantly affect cocaine self-administration under FR2 reinforcement (Fig. S17A–C). As 0.5 mg/kg/infusion cocaine lies on the descending limb of the cocaine dose-response curve [50–54], we next examined whether ivabradine alters cocaine self-administration across a full range of cocaine doses. After 10 days of cocaine self-administration training, rats that met criteria for stable cocaine self-administration were subsequently trained in a single self-administration session maintained by a full range of cocaine doses under a FR2 reinforcement schedule. We observed classic inverted U-shaped dose-response curves, and maximal infusions occurred at the 0.125 mg/kg/infusion dose (Fig. 6B). After rats achieved stable cocaine self-administration in this multiple dose paradigm, ivabradine (25 and 50 ng/0.5 μ l/side) or vehicle was infused into the VTA 10 min prior to cocaine self-administration. Ivabradine led to dose-dependent downward shifts of the cocaine dose-response curve (Fig. 6B). We next examined whether intra-VTA ivabradine alters cocaine self-administration under a progressive ratio (PR) schedule of reinforcement [55]. Intra-VTA infusions of ivabradine dose-dependently reduced cocaine infusions (Fig. 6C) and breakpoints (Fig. 6D) compared to vehicle infusions, suggesting reduced motivation to obtain cocaine when the effort required is progressively increased. The location of cannula implantation was verified after the experiments (Fig. S18).

Effects of systemic injections of ivabradine on cocaine self-administration

We next determined whether systemic HCN blockade also affects motivated drug taking. To test this, rats were trained to self-

administer cocaine under FR1/FR2 for 10 days (1 and 0.5 mg/kg/infusion, Fig. 6A). On subsequent days, we examined the effects of systemic administration of ivabradine or vehicle on cocaine self-administration under a FR2 schedule with 0.5 mg/kg/infusion cocaine. Currently available HCN channel blockers, including ivabradine, show a very limited ability to cross the blood-brain barrier (BBB) due to p-glycoprotein-mediated efflux, unless delivered with the p-glycoprotein inhibitor elacridar [56]. Rats first received an i.v. injection of elacridar (5 mg/kg) followed by an i.p. injection of ivabradine (3 or 10 mg/kg) or vehicle (0 mg/kg) 10 min prior to cocaine self-administration. Ivabradine (with elacridar) dose-dependently reduced active lever presses (Fig. 6E) and cocaine infusions (Fig. 6F) compared to vehicle (with elacridar) but had no significant effect on inactive lever presses (Fig. S19).

We next examined the effects of ivabradine on the cocaine dose response curve in a separate cohort of rats. After acquiring stable cocaine self-administration in the multiple dose paradigm, rats received elacridar (5 mg/kg, i.v.) followed by ivabradine (3 or 10 mg/kg, i.p.) or vehicle (0 mg/kg) injection 10 min prior to multidose cocaine self-administration. Ivabradine pretreatments led to a dose-dependent downward shift in the cocaine dose-response curve and an attenuation of cocaine intake, the shift was more prominent on the ascending limb at the lower dose ivabradine (3 mg/kg; Fig. 6G, H). Finally, we determined whether ivabradine affects the motivation for cocaine self-administration under a PR reinforcement schedule. Elacridar and ivabradine treatments were performed as described above, and the effects of ivabradine (3 or 10 mg/kg, i.p.) or vehicle on cocaine infusions and breakpoint were examined. Ivabradine pretreatment dose-dependently reduced cocaine infusions (Fig. 6I) and breakpoint (Fig. 6J) compared to vehicle-treated rats. Thus, ivabradine reduced the motivation to obtain cocaine when the effort required is progressively increased. Taken together, the above results suggest that ivabradine reduces cocaine intake by decreasing the motivation for cocaine taking.

Effects of systemic injections of ivabradine on oral sucrose self-administration

To determine whether ivabradine affects non-drug reinforcement, we investigated the effects of ivabradine on oral self-administration of sucrose pellets under both FR2 and PR schedules. Rats established stable oral sucrose self-administration during the 10-day training period which emulated the procedure for cocaine self-administration training. On subsequent days, the effects of ivabradine (0, 3 or 10 mg/kg, i.p.) in combination with i.v. injection of elacridar (5 mg/kg) on sucrose self-administration were tested. In contrast to cocaine self-administration, when tested for effects on sucrose self-administration under a FR2 schedule, ivabradine at 3 or 10 mg/kg had no significant effects on active and inactive lever presses or sucrose pellets earned (Fig. S20A–C) compared to vehicle and elacridar. Moreover, while ivabradine reduced sucrose pellet self-administration under the PR schedule, these effects were only observed at the high (i.e., 10 mg/kg) dose at which significant decreases in sucrose pellets earned and breakpoint were found (Fig. S20D, E). In contrast to cocaine self-administration, significant effects of the lower (i.e., 3 mg/kg) ivabradine dose were not observed (Fig. S20D, E). Altogether, these findings demonstrate that ivabradine selectively influences cocaine self-administration, with effects on motivation to obtain a natural reward observed only at a higher ivabradine dose and under conditions where the effort required to obtain the natural reward is greater.

DISCUSSION

Here, we show that both VTA dopamine and GABA neurons expressed cAMP-sensitive HCN mRNA (*Hcn2* and *Hcn4*) and that I_h in these neurons was sensitive to cAMP stimulation. Acute bath

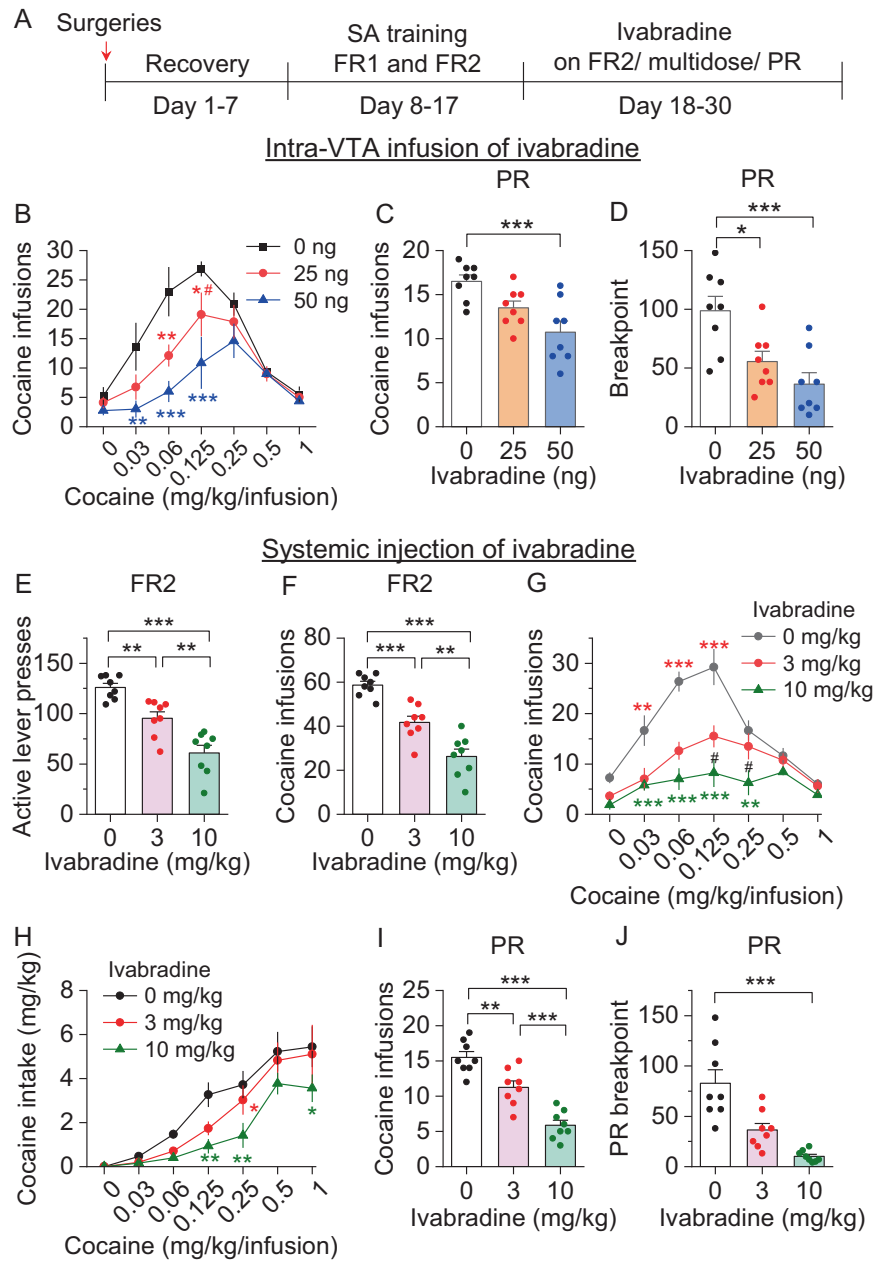


Fig. 6 Ivabradine dose-dependently decreased cocaine intake under FR/PR schedules and produced a downward shift of the cocaine dose-response curve. **A** Timeline of catheterization, cocaine self-administration and ivabradine treatment. **B** Intra-VTA infusion of Ivabradine produced a significant downward shift in the number of cocaine infusions on the cocaine dose-response curve (two-way RM ANOVA: Ivabradine, $F_{2,21} = 13.0$, $p < 0.001$; cocaine dose, $F_{6,126} = 22.0$, $p < 0.001$; Ivabradine \times cocaine dose interaction, $F_{6,126} = 2.5$, $p = 0.005$; 25 ng vs 0 ng, red *; 50 ng vs 0 ng, blue *; 25 ng vs 50 ng, red #; $n = 8$ rats for each group). **C** Intra-VTA infusion of significantly attenuated the number of cocaine infusions under PR reinforcement conditions (one-way ANOVA, $F_{2,21} = 9.1$, $p = 0.001$, $n = 8$ rats in each group). **D** Intra-VTA infusion of significantly attenuated the PR breakpoint (one-way ANOVA, $F_{2,21} = 9.7$, $p = 0.001$, $n = 8$ rats in each group). **E, F** Systemic ivabradine administration (0, 3, 10 mg/kg, i.p.) following iv elacridar (5 mg/kg), dose-dependently decreased the mean number of active lever presses (**E**, one-way ANOVA: $F_{2,23} = 27.3$, $p < 0.001$) and cocaine infusions under an FR2 reinforcement schedule (**F**, one-way ANOVA: $F_{2,23} = 35.6$, $p < 0.001$) ($n = 8$ rats in each group). **G, H** Ivabradine pretreatment produced a significant downward shift in the dose-response curve for cocaine infusions (**G**, two-way RM ANOVA: ivabradine pretreatment, $F_{2,21} = 16.9$, $p < 0.001$; cocaine dose, $F_{6,126} = 28.0$, $p < 0.001$; ivabradine pretreatment \times cocaine dose interaction, $F_{12,126} = 6.3$, $p < 0.001$; 3 vs. 0 mg/kg ivabradine, red *; 10 vs. 0 mg/kg ivabradine, green *; 3 vs. 10 mg/kg ivabradine black #) and decreased total cocaine intake (**H**, two-way RM ANOVA: ivabradine pretreatment, $F_{2,21} = 5.8$, $p = 0.010$; cocaine dose, $F_{6,126} = 68.7$, $p < 0.001$; ivabradine \times cocaine dose interaction, $F_{12,126} = 1.6$, $p = 0.090$; 10 vs. 0 mg/kg ivabradine green *; 3 vs. 10 mg/kg ivabradine red *) on the dose-response curve ($n = 8$ rats in each group). **I, J** Ivabradine dose-dependently decreased the number of cocaine infusions (**I**, one-way ANOVA: $F_{2,23} = 34.2$, $p < 0.001$; $n = 8$ rats in each group) and breakpoint (**J**, Brown-Forsythe equal variance: $p < 0.05$; Kruskal-Wallis one-way ANOVA on ranks: ivabradine, $H = 17.6$, $p < 0.001$; $n = 8$ rats in each group) under a PR reinforcement schedule. * $p < 0.05$, ** $p < 0.01$, *** $p < 0.001$; # $p < 0.05$, ## $p < 0.01$, ### $p < 0.001$.

application of cocaine and chronic self-administration led to opposite changes in the voltage-dependent activation of I_h in VTA dopamine neurons without significantly altering I_h in VTA GABA neurons. As D_2 (*Drd2*) mRNA was predominantly expressed in VTA dopamine neurons, cocaine-induced activation of D_2 receptors and the resultant decrease in cAMP likely contributes to the I_h modulation. In support of this idea, chronic Gi-DREADD stimulation in VTA dopamine neurons mimicked the effect of cocaine self-administration on I_h upregulation. Finally, we demonstrated that intra-VTA or systemic injections of ivabradine reduced cocaine intake at low unitary cocaine doses and the motivation to obtain cocaine when effort demand is high. These results reveal a critical role of HCN channels in regulating motivated cocaine taking.

Major efforts have been directed towards the identification of VTA dopamine and GABA neurons based on electrophysiological criteria. The presence of I_h currents had historically been used as the key criterion for the identification of midbrain dopamine neurons in brain slices. Through a combination of whole-cell recordings, biocytin loading and *post hoc* immunohistochemistry with TH and GAD antibodies, Margolis et al. reported that both VTA dopamine neurons and GABA neurons exhibited I_h currents with comparable amplitude in rat brain slices [37, 40]. We confirmed these findings with TH-tdTomato fluorescent reporter rats and single-cell PCR that provided unequivocal cell type identification of recorded neurons. Immunohistochemistry has shown that HCN2 is expressed in the rat VTA [36] and that HCN4 is expressed in VTA dopamine and GABA neurons [37]. Although earlier whole-brain *in situ* hybridization analysis has shown that all *Hcn1–4* isoforms are expressed in the VTA [57], the specific cell types that express different HCN isoforms have not been identified, and their expression has not been directly compared between cell types. We utilized RNAscope to quantify the expression of *Hcn1–4* mRNA in defined VTA neuron populations. We found that VTA GABA neurons expressed all 4 *Hcn* mRNA isoforms (*Hcn1–4*), while VTA dopamine neurons expressed predominantly *Hcn3–4*. RNAscope allows detection of single mRNA transcripts with high specificity and sensitivity [57]. Our results provide a high-resolution, quantitative comparison of the specific HCN isoforms expressed in two major neuronal types of the VTA and overcomes the sampling size limitation inherent in whole cell recordings. Previous studies have shown that differences in the amplitude of I_h currents in VTA neurons depend on the projection targets [13, 58–61]. Future studies will be carried out to determine *Hcn1–4* mRNA expression in VTA neurons that project to different brain targets.

HCN channels are often assembled as heterotetramers in native neurons [1, 33, 34]. HCN2 and HCN4 are highly sensitive to cAMP, whereas HCN1 and HCN3 are relatively insensitive to cAMP [3, 38, 39]. Both RNAscope and electrophysiological recordings indicate that HCN channels expressed on VTA dopamine and GABA neurons are sensitive to cAMP. Indeed, increasing intracellular cAMP with forskolin and rolipram produced similar depolarizing shifts of $V_{1/2}$ of I_h in VTA dopamine and GABA neurons. However, bath application of cocaine led to D_2 -dependent hyperpolarizing shifts of $V_{1/2}$ in VTA dopamine neurons but did not alter I_h in VTA GABA neurons. D_2 (*Drd2*) mRNA was predominantly expressed in VTA dopamine neurons, whereas D_1 (*Drd1*) mRNA was barely detectable in the VTA, which may explain the lack of significant effects of cocaine on I_h in VTA GABA neurons.

Acute and chronic Gs-DREADD stimulation produced opposite modulation of HCN function in hippocampal CA1 pyramidal neurons and depressive-like behaviors via cAMP-dependent mechanisms [10]. However, whether this cAMP-induced regulation of HCN can be induced by animals' behavioral experiences remained previously unknown. We found that acute bath application of cocaine and chronic cocaine self-administration produced opposite modulation of I_h currents in VTA dopamine

neurons but did not alter I_h in VTA GABA neurons. Several lines of evidence suggest that a chronic decrease in cAMP via D_2 receptor activation mediates the I_h modulation in the VTA dopamine neurons. First, *Drd2* mRNA is predominantly expressed in dopamine neurons, while cocaine alters I_h only in dopamine neurons. Second, we found that yoked cocaine infusions and chronic Gi-DREADD stimulation also led to an upregulation of I_h currents in VTA dopamine neurons. Thus, all three manipulations that induced a chronic decrease in cAMP in dopamine neurons caused a similar upregulation of I_h currents and reduced temporal summation of EPSPs, suggesting a common mechanism. However, it is important to acknowledge that genetically engineered receptors are unlikely to fully replicate the complex mechanisms of endogenous receptor activation.

The auxiliary subunit TRIP8b is required for the trafficking of HCN channels to the membrane surface and enrichment at dendrites [44, 48]. TRIP8b competes with cAMP for binding of HCN channels via an allosteric inhibitory mechanism [62–64]. Chronic Gs-DREADD stimulation in hippocampal CA1 pyramidal neurons impaired HCN cell surface trafficking via disruption of TRIP8b-HCN interactions [10]. As TRIP8b is highly enriched in midbrain dopamine neurons (Fig. S14), it is likely that chronically decreased cAMP causes increased TRIP8b-HCN interaction, resulting in increased HCN channel cell surface trafficking. In support of this idea, we have shown that chronic hM4D(Gi) stimulation led to an increase in TRIP8b binding to HCN3 and HCN4 in the VTA. Increased HCN trafficking to the cell membrane and dendrites of VTA dopamine neurons likely underlies the observed decrease in temporal summation of EPSPs via decreased input resistance.

Our findings that cocaine self-administration induced an upregulation of I_h currents stand in contrast to an earlier study showing that 7 days of cocaine (15 mg/kg) i.p. injections in rats decreased I_h amplitude in putative VTA dopamine neurons by ~40%, which was accompanied by a reduction in cell capacitance of similar magnitude (~33%), leaving I_h density unaltered [65]. Although we cannot exclude the possibility that i.p. cocaine injections and i.v. cocaine administration produced differential modulation of I_h currents in VTA dopamine neurons, other factors may contribute to the differences. Of note, VTA neurons in that study were identified as dopaminergic only by the presence of I_h currents, and the minimum threshold value for I_h amplitude was not defined [65]. Studying changes in I_h currents in dopamine neurons while concurrently using I_h as a marker for neuron identification may introduce potential bias and sampling error. Indeed, the averaged I_h current amplitude in the saline group was ~500 pA at -130 mV [65], which was considerably larger than the I_h currents in our saline group and those previously reported in drug-naïve rats [40]. Additionally, i.p. injection of cocaine for 7 days leads to a 33% decrease in membrane capacitance [65]. As there is a linear relationship between cell capacitance and membrane surface area [66], the decrease in cell capacitance was interpreted as a decrease in soma size of VTA dopamine neurons [65]. However, both the present and a prior study [67] found that cocaine self-administration did not significantly change the soma size of VTA dopamine neurons as determined by TH immunofluorescence as well as cell capacitance.

HCN channels are abundantly expressed in the VTA, yet it was previously unknown whether HCN channels contribute to motivated drug taking behavior. As chronic cocaine self-administration upregulated I_h currents in VTA dopamine neurons, we tested whether a clinically approved HCN blocker could reduce cocaine self-administration. Ivabradine is a nonselective blocker of all 4 HCN isoforms [68, 69] and does not produce significant off-target effects on voltage-gated Na^+ , Ca^{2+} , and K^+ channels at concentrations that block HCN channels [70, 71]. We found that intra-VTA infusion of ivabradine produced a dose-dependent suppression of cocaine intake on a PR schedule and a downward shift of the cocaine dose-response curve. The decrease in operant

responding on the ascending limb could be attributable to a decrease in the reinforcing efficacy of cocaine [72–74]. Cocaine-induced increases in dopamine levels in the striatum contribute to its reinforcing effects [16, 75]. Dopamine release is triggered by AP firing in dopamine neurons. HCN blockers significantly decreased spontaneous AP firing in these neurons [13–15]. HCN blockade is expected to decrease dopamine release in the NAc, which may explain the common decrease in operant responding when cocaine unitary doses were relatively low or when the effort required to obtain cocaine reward was progressively increased under PR reinforcement. However, intra-VTA infusion of ivabradine did not significantly affect the FR2 reinforcement schedule at 0.5 mg/kg/infusion and the descending limb of the inverted U-shaped dose-response curve, suggesting that higher unitary doses of cocaine remain similarly reinforcing despite HCN blockade. Ivabradine blocks HCN channels in the VTA non-discriminately. It is possible that HCN blockade in non-dopamine neurons may also contribute to the effects of ivabradine on cocaine intake.

Systemic injection of ivabradine produced similar effects on cocaine self-administration compared with intra-VTA ivabradine while producing an additional suppression of cocaine intake under a FR2 schedule. Ivabradine produced a downward, but not a rightward, shift of the cocaine dose response curve, suggesting that the reduction of the reinforcing strength of cocaine by ivabradine may not be compensated by increasing the amount of drug used per occasion. This feature is advantageous from a therapeutic perspective, as one cannot overcome the effect by taking greater cocaine doses [73]. Ivabradine is clinically approved for the treatment of heart failure [20, 21], and heart failure secondary to dilated cardiomyopathy is the leading cause of death in long-term cocaine users [19]. Cocaine increases heart rate and blood pressure via inhibition of catecholamine reuptake [76], while ivabradine is well tolerated and causes minimal side effects such as bradycardia [77]. Brain penetrant isoform-specific HCN blockers have also been developed and were shown to protect against seizures in mice [36]. Small-molecule inhibitors of the TRIP8b-HCN interaction may provide more selective targeting of neuronal HCNs [78]. There is therefore an opportunity to target HCNs for the treatment of cocaine use disorder and other mental disorders such as depression.

DATA AVAILABILITY

All data supporting the findings of this study are documented within the paper and Supplementary materials, additional data are available from the corresponding author upon reasonable request. We have provided Source Data in Supplementary materials and statistical conclusion in figure legends.

REFERENCES

- Wahl-Schott C, Biel M. HCN channels: structure, cellular regulation and physiological function. *Cell Mol Life Sci: CMLS*. 2009;66:470–94.
- Robinson RB, Siegelbaum SA. Hyperpolarization-activated cation currents: from molecules to physiological function. *Annu Rev Physiol*. 2003;65:453–80.
- Wainger BJ, DeGennaro M, Santoro B, Siegelbaum SA, Tibbs GR. Molecular mechanism of cAMP modulation of HCN pacemaker channels. *Nature*. 2001;411:805–10.
- Chen S, Wang J, Siegelbaum SA. Properties of hyperpolarization-activated pacemaker current defined by coassembly of HCN1 and HCN2 subunits and basal modulation by cyclic nucleotide. *J Gen Physiol*. 2001;117:491–504.
- Brown HF, DiFrancesco D, Noble SJ. How does adrenaline accelerate the heart? *Nature*. 1979;280:235–6.
- DiFrancesco D. The onset and autonomic regulation of cardiac pacemaker activity: relevance of the f current. *Cardiovasc Res*. 1995;29:449–56.
- Wang M, Ramos BP, Paspalas CD, Shu Y, Simen A, Duque A, et al. Alpha2A-adrenoceptors strengthen working memory networks by inhibiting cAMP-HCN channel signaling in prefrontal cortex. *Cell*. 2007;129:397–410.
- Harris NA, Isaac AT, Günther A, Merkel K, Melchior J, Xu M, et al. Dorsal BNST $\alpha(2A)$ -Adrenergic Receptors Produce HCN-Dependent Excitatory Actions That Initiate Anxiogenic Behaviors. *J Neurosci*. 2018;38:8922–42.
- Emery EC, Young GT, Berrococo EM, Chen L, McNaughton PA. HCN2 ion channels play a central role in inflammatory and neuropathic pain. *Science* (New York, NY). 2011;333:1462–6.
- Lyman KA, Han Y, Zhou C, Renteria I, Besing GL, Kurz JE, et al. Hippocampal cAMP regulates HCN channel function on two time scales with differential effects on animal behavior. *Sci Transl Med*. 2021;13:eabl4580.
- Tsantoulas C, Lainez S, Wong S, Mehta I, Vilar B, McNaughton PA. Hyperpolarization-activated cyclic nucleotide-gated 2 (HCN2) ion channels drive pain in mouse models of diabetic neuropathy. *Sci Transl Med*. 2017;9:eaam6072.
- Morales M, Margolis EB. Ventral tegmental area: cellular heterogeneity, connectivity and behaviour. *Nat Rev*. 2017;18:73–85.
- Friedman AK, Walsh JJ, Juarez B, Ku SM, Chaudhury D, Wang J, et al. Enhancing depression mechanisms in midbrain dopamine neurons achieves homeostatic resilience. *Science* (New York, NY). 2014;344:313–9.
- Okamoto T, Harnett MT, Morikawa H. Hyperpolarization-activated cation current (I_h) is an ethanol target in midbrain dopamine neurons of mice. *J Neurophysiol*. 2006;95:619–26.
- McDaid J, McElvain MA, Brodie MS. Ethanol effects on dopaminergic ventral tegmental area neurons during block of I_h: involvement of barium-sensitive potassium currents. *J Neurophysiol*. 2008;100:1202–10.
- Anderson SM, Pierce RC. Cocaine-induced alterations in dopamine receptor signaling: implications for reinforcement and reinstatement. *Pharmacol Ther*. 2005;106:389–403.
- Ford CP. The role of D2-autoreceptors in regulating dopamine neuron activity and transmission. *Neuroscience*. 2014;282:13–22.
- Tritsch NX, Sabatini BL. Dopaminergic modulation of synaptic transmission in cortex and striatum. *Neuron*. 2012;76:33–50.
- Felker GM, Hu W, Hare JM, Hruban RH, Baughman KL, Kasper EK. The spectrum of dilated cardiomyopathy. The Johns Hopkins experience with 1,278 patients. *Med* (Baltim). 1999;78:270–83.
- Postea O, Biel M. Exploring HCN channels as novel drug targets. *Nat Rev Drug Discov*. 2011;10:903–14.
- Fala L. Corlanor (Ivabradine), First HCN Channel Blocker, FDA approved for the treatment of patients with heart failure. *Am Health Drug Benefits*. 2016;9:56–9.
- Witten IB, Steinberg EE, Lee SY, Davidson TJ, Zalocusky KA, Brodsky M, et al. Recombinase-driver rat lines: tools, techniques, and optogenetic application to dopamine-mediated reinforcement. *Neuron*. 2011;72:721–33.
- Vickstrom CR, Liu X, Liu S, Hu MM, Mu L, Hu Y, et al. Role of endocannabinoid signaling in a septohabenular pathway in the regulation of anxiety- and depressive-like behavior. *Mol Psychiatry*. 2021;26:3178–91.
- Vickstrom CR, Liu X, Zhang Y, Mu L, Kelly TJ, Yan X, et al. T-Type Calcium Channels Contribute to Burst Firing in a Subpopulation of Medial Habenula Neurons. *eNeuro* 2020;7:0201–20.
- Mu L, Liu X, Yu H, Hu M, Friedman V, Kelly TJ, et al. Ibudilast attenuates cocaine self-administration and prime- and cue-induced reinstatement of cocaine seeking in rats. *Neuropharmacology*. 2021;201:108830.
- Ting JT, Lee BR, Chong P, Soler-Llavina G, Cobbs C, Koch C, et al. Preparation of acute brain slices using an optimized N-Methyl-D-glucamine protective recovery method. *J Visualized Exp. JoVE*. 2018;26:53825.
- Zhong P, Vickstrom CR, Liu X, Hu Y, Yu L, Yu HG, et al. HCN2 channels in the ventral tegmental area regulate behavioral responses to chronic stress. *Elife* 2018;7:e32420. <https://doi.org/10.7554/eLife.32420>.
- Yu H, Liu X, Chen B, Vickstrom CR, Friedman V, Kelly TJ, et al. The Neuroprotective Effects of the CB2 Agonist GW842166x in the 6-OHDA Mouse Model of Parkinson's Disease. *Cells* 2021;10:3548.
- Wright KN, Strong CE, Addonizio MN, Brownstein NC, Kabbaj M. Reinforcing properties of an intermittent, low dose of ketamine in rats: effects of sex and cycle. *Psychopharmacology*. 2017;234:393–401.
- Zhong P, Wang W, Yu F, Nazari M, Liu X, Liu QS. Phosphodiesterase 4 inhibition impairs cocaine-induced inhibitory synaptic plasticity and conditioned place preference. *Neuropsychopharmacology*. 2012;37:2377–87.
- Liu X, Liu Y, Zhong P, Wilkinson B, Qi J, Olsen CN, et al. CaMKII activity in the ventral tegmental area gates cocaine-induced synaptic plasticity in the nucleus accumbens. *Neuropsychopharmacology*. 2014;39:989–99.
- Liu X, Vickstrom CR, Yu H, Liu S, Snarrenberg ST, Friedman V, et al. Epac2 in midbrain dopamine neurons contributes to cocaine reinforcement via enhancement of dopamine release. *Elife* 2022;11:e80747.
- Santoro B, Liu DT, Yao H, Bartsch D, Kandel ER, Siegelbaum SA, et al. Identification of a gene encoding a hyperpolarization-activated pacemaker channel of brain. *Cell*. 1998;93:171–29.
- Ludwig A, Zong X, Hofmann F, Biel M. Structure and function of cardiac pacemaker channels. *Cell Physiol Biochem*. 1999;9:179–86.
- Monteggia LM, Eisch AJ, Tang MD, Kaczmarek LK, Nestler EJ. Cloning and localization of the hyperpolarization-activated cyclic nucleotide-gated channel family in rat brain. *Brain Res Mol Brain Res*. 2000;81:129–39.

36. Notomi T, Shigemoto R. Immunohistochemical localization of Ih channel subunits, HCN1-4, in the rat brain. *J Comp Neurol.* 2004;471:241–76.
37. Margolis EB, Toy B, Himmels P, Morales M, Fields HL. Identification of rat ventral tegmental area GABAergic neurons. *PLoS one.* 2012;7:e42365.
38. Wang J, Chen S, Siegelbaum SA. Regulation of hyperpolarization-activated HCN channel gating and cAMP modulation due to interactions of COOH terminus and core transmembrane regions. *J Gen Physiol.* 2001;118:237–50.
39. Stieber J, Stockl G, Herrmann S, Hassfurth B, Hofmann F. Functional expression of the human HCN3 channel. *J Biol Chem.* 2005;280:34635–43.
40. Margolis EB, Lock H, Hjelmstad GO, Fields HL. The ventral tegmental area revisited: is there an electrophysiological marker for dopaminergic neurons? *J Physiol.* 2006;577:907–24.
41. Liu X, Zhong P, Vickstrom C, Li Y, Liu QS. PDE4 inhibition restores the balance between excitation and inhibition in VTA dopamine neurons disrupted by repeated in vivo cocaine exposure. *Neuropsychopharmacology.* 2017;42:1991–9.
42. McCall NM, Marron Fernandez de Velasco E, Wickman K. GIRK channel activity in dopamine neurons of the ventral tegmental area bidirectionally regulates behavioral sensitivity to cocaine. *J Neurosci.* 2019;39:3600–10.
43. Magee JC. Dendritic Ih normalizes temporal summation in hippocampal CA1 neurons. *Nat Neurosci.* 1999;2:848.
44. Lewis AS, Vaidya SP, Blaiss CA, Liu Z, Stoub TR, Brager DH, et al. Deletion of the hyperpolarization-activated cyclic nucleotide-gated channel auxiliary subunit TRIP8b impairs hippocampal Ih localization and function and promotes antidepressant behavior in mice. *J Neurosci.* 2011;31:7424–40.
45. Juarez B, Han MH. Diversity of dopaminergic neural circuits in response to drug exposure. *Neuropsychopharmacology.* 2016;41:2424–46.
46. Tye KM, Mirzabekov JJ, Warden MR, Ferencci EA, Tsai HC, Finkelstein J, et al. Dopamine neurons modulate neural encoding and expression of depression-related behaviour. *Nature.* 2013;493:537–41.
47. Santoro B, Wainger BJ, Siegelbaum SA. Regulation of HCN channel surface expression by a novel C-terminal protein-protein interaction. *J Neurosci.* 2004;24:10750–62.
48. Han Y, Lyman KA, Foote KM, Chetkovich DM. The structure and function of TRIP8b, an auxiliary subunit of hyperpolarization-activated cyclic-nucleotide-gated channels. *Channels.* 2020;14:110–22.
49. Nagai Y, Miyakawa N, Takuwa H, Hori Y, Oyama K, Ji B, et al. Deschloroclozapine, a potent and selective chemogenetic actuator enables rapid neuronal and behavioral modulations in mice and monkeys. *Nat Neurosci.* 2020;23:1157–67.
50. Caine SB, Thomsen M, Gabriel KI, Berkowitz JS, Gold LH, Koob GF, et al. Lack of self-administration of cocaine in dopamine D1 receptor knock-out mice. *J Neurosci.* 2007;27:13140–50.
51. Arnold JM, Roberts DC. A critique of fixed and progressive ratio schedules used to examine the neural substrates of drug reinforcement. *Pharmacol, Biochem, Behav.* 1997;57:441–7.
52. Barrett AC, Miller JR, Dohrmann JM, Caine SB. Effects of dopamine indirect agonists and selective D1-like and D2-like agonists and antagonists on cocaine self-administration and food maintained responding in rats. *Neuropharmacology.* 2004;47:256–73.
53. Song R, Zhang HY, Li X, Bi GH, Gardner EL, Xi ZX. Increased vulnerability to cocaine in mice lacking dopamine D3 receptors. *Proc Natl Acad Sci USA.* 2012;109:17675–80.
54. Zhang HY, Bi GH, Yang HJ, He Y, Xue G, Cao J, et al. The Novel Modafinil Analog, JJC8-016, as a Potential Cocaine Abuse Pharmacotherapeutic. *Neuropsychopharmacology.* 2017;42:1871–83.
55. Hodos W. Progressive ratio as a measure of reward strength. *Science (New York, NY).* 1961;134:943–4.
56. Iacone Y, Morais TP, David F, Delicata F, Sandle J, Raffai T, et al. Systemic administration of ivabradine, a hyperpolarization-activated cyclic nucleotide-gated channel inhibitor, blocks spontaneous absence seizures. *Epilepsia.* 2021;62:1729–43.
57. Wang F, Flanagan J, Su N, Wang LC, Bui S, Nielson A, et al. RNAscope: a novel in situ RNA analysis platform for formalin-fixed, paraffin-embedded tissues. *J Mol Diagnostics: JMD.* 2012;14:22–9.
58. Margolis EB, Lock H, Chefer VI, Shippenberg TS, Hjelmstad GO, Fields HL. Kappa opioids selectively control dopaminergic neurons projecting to the prefrontal cortex. *Proc Natl Acad Sci USA.* 2006;103:2938–42.
59. Lammel S, Ion DI, Roeper J, Malenka RC. Projection-specific modulation of dopamine neuron synapses by aversive and rewarding stimuli. *Neuron.* 2011;70:855–62.
60. Lammel S, Hetzel A, Hackel O, Jones I, Liss B, Roeper J. Unique properties of mesoprefrontal neurons within a dual mesocorticolimbic dopamine system. *Neuron.* 2008;57:760–73.
61. Ford CP, Mark GP, Williams JT. Properties and opioid inhibition of mesolimbic dopamine neurons vary according to target location. *J Neurosci.* 2006;26:2788–97.
62. Santoro B, Piskrowski RA, Pian P, Hu L, Liu HY, Siegelbaum SA. TRIP8b Splice Variants Form a Family of Auxiliary Subunits that Regulate Gating and Trafficking of HCN Channels in the Brain. *Neuron.* 2009;62:802–13.
63. Lewis AS, Schwartz E, Chan CS, Noam Y, Shin M, Wadman WJ, et al. Alternatively spliced isoforms of TRIP8b differentially control h channel trafficking and function. *J Neurosci.* 2009;29:6250–65.
64. Saponaro A, Cantini F, Porro A, Bucchi A, DiFrancesco D, Maione V, et al. A synthetic peptide that prevents cAMP regulation in mammalian hyperpolarization-activated cyclic nucleotide-gated (HCN) channels. *Elife.* 2018;7:e35753.
65. Arencibia-Albite F, Vazquez R, Velasquez-Martinez MC, Jimenez-Rivera CA. Cocaine sensitization inhibits the hyperpolarization-activated cation current Ih and reduces cell size in dopamine neurons of the ventral tegmental area. *J Neurophysiol.* 2012;107:2271–82.
66. Kado RT. Membrane area and electrical capacitance. *Methods Enzymol.* 1993;221:273–99.
67. Mazei-Robison MS, Appasani R, Edwards S, Wee S, Taylor SR, Picciotto MR, et al. Self-administration of ethanol, cocaine, or nicotine does not decrease the soma size of ventral tegmental area dopamine neurons. *PLoS one.* 2014;9:e95962.
68. Bucchi A, Tognati A, Milanese R, Baruscotti M, DiFrancesco D. Properties of ivabradine-induced block of HCN1 and HCN4 pacemaker channels. *J Physiol.* 2006;572:335–46.
69. Stieber J, Wieland K, Stöckl G, Ludwig A, Hofmann F. Bradycardic and proarrhythmic properties of sinus node inhibitors. *Mol Pharm.* 2006;69:1328–37.
70. Bois P, Bescond J, Renaudon B, Lenfant J. Mode of action of bradycardic agent, S 16257, on ionic currents of rabbit sinoatrial node cells. *Br J Pharmacol.* 1996;118:1051–7.
71. Young GT, Emery EC, Mooney ER, Tsantoulas C, McNaughton PA. Inflammatory and neuropathic pain are rapidly suppressed by peripheral block of hyperpolarisation-activated cyclic nucleotide-gated ion channels. *Pain.* 2014;155:1708–19.
72. Roberts DC, Gabriele A, Zimmer BA. Conflation of cocaine seeking and cocaine taking responses in IV self-administration experiments in rats: methodological and interpretational considerations. *Neurosci Biobehav Rev.* 2013;37:2026–36.
73. Mello NK, Negus SS. Preclinical evaluation of pharmacotherapies for treatment of cocaine and opioid abuse using drug self-administration procedures. *Neuropsychopharmacology.* 1996;14:375–424.
74. Caine SB, Negus SS, Mello NK, Patel S, Bristow L, Kulagowski J, et al. Role of dopamine D2-like receptors in cocaine self-administration: studies with D2 receptor mutant mice and novel D2 receptor antagonists. *J Neurosci.* 2002;22:2977–88.
75. Volkow ND, Wang GJ, Telang F, Fowler JS, Logan J, Childress AR, et al. Cocaine cues and dopamine in dorsal striatum: mechanism of craving in cocaine addiction. *J Neurosci.* 2006;26:6583–8.
76. Kim ST, Park T. Acute and chronic effects of cocaine on cardiovascular health. *Int J Mol Sci.* 2019;20:584.
77. Savelieva I, Camm AJ. f inhibition with ivabradine: electrophysiological effects and safety. *Drug Saf.* 2008;31:95–107.
78. Han Y, Iyamu ID, Clutter MR, Mishra RK, Lyman KA, Zhou C, et al. Discovery of a small-molecule inhibitor of the TRIP8b-HCN interaction with efficacy in neurons. *J Biol Chem.* 2022;298:102069.

ACKNOWLEDGEMENTS

This work was supported by National Institutes of Health Grants R01DA035217 and R01DA047269 (to QSL), F30MH115536 (to CRV) and F31DA054759 (to VF). CRV and TJK are members of the Medical Scientist Training Program at MCW, which is partially supported by a training grant from NIGMS T32-GM080202.

AUTHOR CONTRIBUTIONS

ML, XL, CRV, QSL, and JM designed the experiments. ML, XL, HY, CRV, VF, TJK, YH, WS, and SL performed experiments and data analysis; ML, XJ, CRV, VF, QSL, and JM wrote the manuscript.

COMPETING INTERESTS

The authors declare no competing interests.

ADDITIONAL INFORMATION

Supplementary information The online version contains supplementary material available at <https://doi.org/10.1038/s41380-023-02290-x>.

Correspondence and requests for materials should be addressed to Qing-song Liu.

Reprints and permission information is available at <http://www.nature.com/reprints>

Publisher's note Springer Nature remains neutral with regard to jurisdictional claims in published maps and institutional affiliations.



Open Access This article is licensed under a Creative Commons Attribution 4.0 International License, which permits use, sharing, adaptation, distribution and reproduction in any medium or format, as long as you give appropriate credit to the original author(s) and the source, provide a link to the Creative Commons licence, and indicate if changes were made. The images or other third party material in this article are included in the article's Creative Commons licence, unless indicated otherwise in a credit line to the material. If material is not included in the article's Creative Commons licence and your intended use is not permitted by statutory regulation or exceeds the permitted use, you will need to obtain permission directly from the copyright holder. To view a copy of this licence, visit <http://creativecommons.org/licenses/by/4.0/>.

© The Author(s) 2023